

Eoarchean/Hadean melts reveal arc-like trace element and isotopic chemistry

Wriju Chowdhury (✉ wchowdhu@ur.rochester.edu)

University of Rochester

Dustin Trail

University of Rochester <https://orcid.org/0000-0003-3505-4351>

Martha Miller

University of Rochester

Paul Savage

University of St. Andrews

Article

Keywords:

Posted Date: May 31st, 2022

DOI: <https://doi.org/10.21203/rs.3.rs-1610334/v1>

License: © ⓘ This work is licensed under a Creative Commons Attribution 4.0 International License.

[Read Full License](#)

Eoarchean/Hadean melts reveal arc-like trace element and isotopic chemistry

Wriju Chowdhury^{1*}, Dustin Trail¹, Martha Miller¹, Paul Savage²

¹ Department of Earth & Environmental Sciences, University of Rochester, Rochester, NY 14627, USA.

² School of Earth and Environmental Sciences, University of St Andrews, Irvine Building, Scotland KY16 9AL, UK

*Corresponding author: Wriju Chowdhury (wchowdhu@ur.rochester.edu)

Summary (193 words)

Constraining the lithological diversity and geodynamic regime(s) of the earliest Earth is critical to understanding how our planet has evolved, and the discovery of Hadean- and Eoarchean-age zircons has allowed us to directly analyse material from these eons. Here we use Jack Hills Zircon (JHZ) (3.3 - 4.2 Ga) analyses coupled with new experimental partitioning data to model the SiO₂ wt.%, Si+O isotopic composition, and trace element (TE) contents of their parent melts; i.e., the composition of the Earth's earliest crust. Comparing our derived JHZ parent melt Si+O isotopic compositions ($-1.96 \leq \delta^{30}\text{Si}_{\text{NBS28}} \leq 0.39 \text{ ‰}$; $5.28 \leq \delta^{18}\text{O}_{\text{VSMOW}} \leq 10.03 \text{ ‰}$) to younger continental crust lithologies, we conclude that the chemistry of the JHZ parent melts was influenced by the assimilation of serpentinites, cherts and silicified basalts, followed by igneous differentiation, leading to the formation of intermediate to felsic melts in the early Earth. Trace element measurements also show that the formational regime had an arc-like chemistry, consistent with the presence of mobile-lid tectonics in the Hadean. Moreover, based on the similarity of isotopic data derived for Eoarchean and Hadean melts, we propose these continental-crust forming processes operated continuously, and uniformly, from the Hadean into the Archaean.

Main (2338 words)

The paucity of terrestrial geological samples from the Hadean and Eoarchean means that making direct inferences about the geochemical and geodynamic nature of the first 500 million years of our planet is

26 fraught with controversy. Many researchers have made implicative arguments about the Hadean through
27 the chemical and isotopic analysis of Hadean zircons and their mineral inclusions. This includes
28 inferences about the types of geodynamic regimes and geological processes that could generate silicic
29 melts (i.e. the earliest continental crust), hydrosphere-lithosphere interactions, and possible mobile-lid
30 tectonics during a time when life may have evolved on our planet¹⁻⁷. Even with access to ancient zircons,
31 the presence or absence of mobile lid tectonics in the Hadean remains a vexed question, with arguments
32 derived to support both end-members. While many have proposed a stagnant-lid for the Hadean Earth
33 based on Hf, O and Nd isotopes⁸⁻¹¹ there are compelling arguments based on geophysical modeling, Nd
34 isotopic evolution models, trace element chemistry of Hadean zircons and Ti isotopic values of the Acasta
35 Gneiss rocks that point toward a mobile-lid regime on the early Earth^{6, 12-17}. Ultimately, these end-
36 member models based on contradictory, but empirical, observations need to be reconciled to provide us
37 with an accurate view of early Earth's geological history.

38 Here we use in-situ analyses of Jack Hills Zircons (JHZs), to place quantitative constraints on the
39 chemistry of their parental magmas, in terms of their trace (TE) and rare-earth (REE) elemental
40 concentrations, SiO₂ content, and Si+O isotopic values. Quantifying SiO₂ content and Si+O isotopes are
41 especially important given that they constitute ~75 wt. % of rock-forming elements in the crust and
42 constitute a majority of the weathered and eroded material that makes up a significant portion of the
43 oceans' nutrient budget. The degree of polymerisation of Si-O bonds also correlates with the relative
44 density of the continental and oceanic crusts which controls long-term continental stability and rock-
45 recycling. Additionally, we also explore the Al content of our zircons which is the third most abundant
46 element in the crust and thus gives us insight into the aluminosity of the parent melts. Aluminosity of
47 melts is of interest because it implies the incorporation of eroded stable subaerial crustal material (See
48 Supplementary information).

49 JHZ parental melt modelling

50 To derive the SiO₂ content and Si+O isotopic values of our zircons' parental melts, we first model their
51 parental melt trace element chemistry by combining in-situ zircon analyses and new experimentally-
52 derived partition coefficients. Then, using melt Th/Y ratio as a proxy for SiO₂ content (whereby Th/Y was
53 calibrated to melt wt% SiO₂ using whole-rock data of lithologies from the GEOROC database), we
54 calculate the wt% SiO₂ concentration of JHZ parent melts⁶. The JHZ crystallization temperatures were
55 estimated using the Ti-in-zircon thermometer^[18]. The derived melt temperature and SiO₂ content both
56 control zircon-melt Si and O isotope fractionation factors^[19, 20]. The fractionation factors combined with
57 in-situ zircon Si and O isotopic measurements are used to derive the melt Si and O compositions. Using
58 this approach, we estimate the Si and O isotopic melt values for each individual Hadean and Eoarchean
59 zircon analysed, which we use as a petrological descriptor of early Earth crustal lithologies. Specifically,
60 individual JHZ melt Si+O isotopic values can identify if supracrustal or altered sources, such as clays,
61 shales, serpentinites, cherts, and/or silicified pillow basalts could have been involved in the formation of
62 the aforementioned melts (while O isotopes in serpentinites have been well studied, Si isotopes for the
63 same are not and so we also present new Si isotopic data from modern serpentinites). Ultimately, each
64 JHZ analysis provides constraints on a parental melt's SiO₂ wt%, TE/REE, and Si/O isotope
65 compositions, which allows us to infer the possible lithological and tectonic character of these zircon-
66 bearing Hadean rocks.

67 JHZ parent melt silica content

68 Silicate melt Th/Y are well correlated with the SiO₂ content of whole rocks⁶ (details and caveats
69 discussed in Online methods), which we use to derive the melt silica content. As noted, we require the
70 SiO₂ content of the Eoarchean/Hadean melts to derive the isotopic chemistry of the same. We measured
71 the concentration of Th and Y of JHZs as a proxy for the melt Th and Y concentration. For these zircon
72 data to be useful, we require zircon-melt partition coefficients (i.e., concentration in zircon divided by
73 concentration in melt; $D_{element}^{zrc/melt}$) to constrain the TE/REE chemistry of the detrital JHZ melts. We
74 conducted new zircon-melt partitioning experiments in an alkali- and water-bearing system and report D-

75 values for Th and Y of 0.72 ± 0.19 (2 s.e.) and 2.90 ± 0.61 respectively, which were used to derive the
 76 Eoarchaean and Hadean melt Th and Y concentrations (See online methods for details; Table ST1). Our
 77 calculated Th and Y concentrations were combined with an empirical calibration (See Online methods) to
 78 estimate melt SiO₂ (Fig 1; Table ST2). The calculated SiO₂ contents range from 51 to 76 wt% with an
 79 average value of 62 ± 11 wt% (2 s.d.) which suggests that most of the melts in question are between
 80 intermediate and felsic. In fact, all our accepted analyses except for two are above 55 wt% SiO₂ (15 of 84
 81 rejected; see Online methods for rejection criteria). Finally, we used the Ti-in-zircon crystallization
 82 thermometer¹⁸ to determine zircon crystallization temperature (Fig S2). The crystallization temperatures

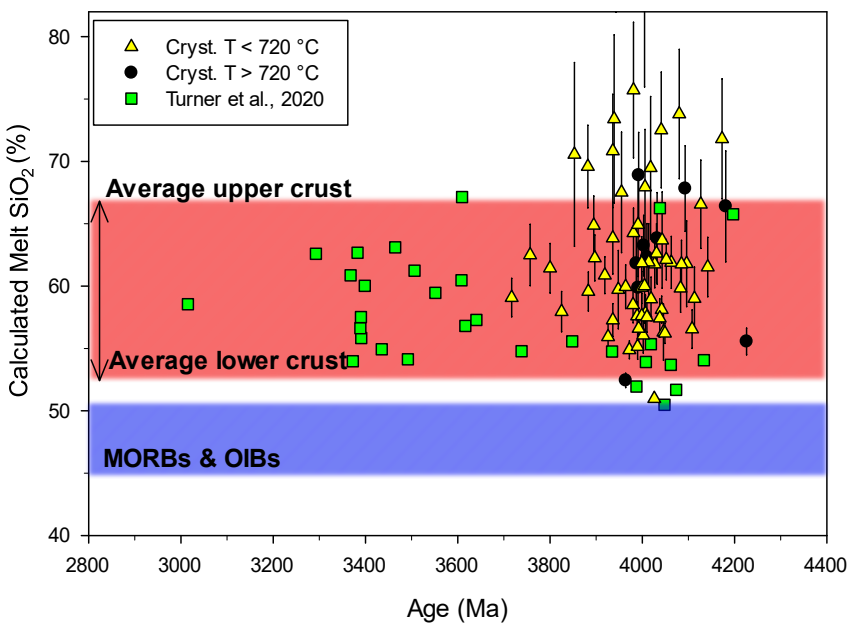


Figure 1. Calculated melt SiO₂ wt% of Hadean and Eoarchaean melts shown against zircon ²⁰⁷Pb-²⁰⁶Pb age. The melt SiO₂ contents are calculated using new trace element partition coefficients reported here and are subtly higher (62 ± 11 wt% (2 s.d.)) than those reported in [6] (58 ± 12 wt% (2 s.d.)), who used D-values reported by [33]. **Field legend:** Red field: The upper bound is the average upper continental crust and the lower bound is the average lower continental crust. Blue field: All MORBs (Mid-Oceanic Ridge Basalts) and OIB (Ocean Island Basalt) values. The upper and lower crust values are from [34]. MORB and OIB values from [29]. Error bars are 2 s.e. (Details in Online Methods). Two zircons with apparent SiO₂ wt% melt values of 99.5% and 91% are not shown.

83 range from 614°C – 774°C with an average of 685 ± 68 °C (2 s.d.) (Fig. S2(B)). Figure 1 and S2(B) both
 84 indicate that most of our JHZs crystallized from water-saturated felsic melts. With these parameters
 85 defined, we can derive the melt $\delta^{30}\text{Si}$ and $\delta^{18}\text{O}$ values.

86 JHZ parent melt isotopic content

87 We performed in-situ coupled $^{30}\text{Si}/^{28}\text{Si}$ and $^{18}\text{O}/^{16}\text{O}$ SIMS measurements on our JHZs (Fig S1; Table
88 ST3). These measurements are necessary to derive the parent melt isotopic content (Table ST4) using
89 fractionation factors. Along with temperature, the primary melt property that affects mineral-melt
90 fractionation factors is the melt silica content and the resulting polymerization of Si-O bonds ^{19,21}. Thus,
91 the derived chemical parameters from the previous section (SiO_2 wt % and crystallization T) allows us to
92 obtain zircon-melt fractionation factors for Si and O isotopes using experimental and empirical
93 calibrations^{19,20} (see online methods), and thereafter the Si and O isotopic composition of the melt. These
94 modelled melt data are far more implicative for deconvolving the petrogenesis of Hadean melts, as we
95 can now compare these isotopic compositions to possible source lithologies (rather than just zircon data
96 alone, see Extended data figures).

97 JHZ parent melt constituents and formational regime

98 In a $\delta^{30}\text{Si}$ vs. $\delta^{18}\text{O}$ plot, we compare our parent melt Si and O isotopic values to potential source
99 lithologies, as well as end-member mantle reservoirs (EM1 (Enriched Mantle 1), EM2 (Enriched Mantle
100 2) and HIMU (High- μ)) and Archaean komatiites (Fig. 2) to quantify possible interacting reservoirs and
101 lithologies that could have created our JHZ melts. An important assumption is that the Phanerozoic and
102 more recent lithologies plotted in Fig. 2 are chemically analogous to similar rocks formed in the Archaean
103 and Hadean. The similarity of Archaean komatiites to modern serpentinites from ODP holes 1268A and
104 1274A (Table ST4) as well as mantle reservoirs indicate hydrothermal processes that alter mantle
105 lithologies alone cannot account for the JHZ melt values and thus lithologies with elevated $\delta^{30}\text{Si}$ and $\delta^{18}\text{O}$

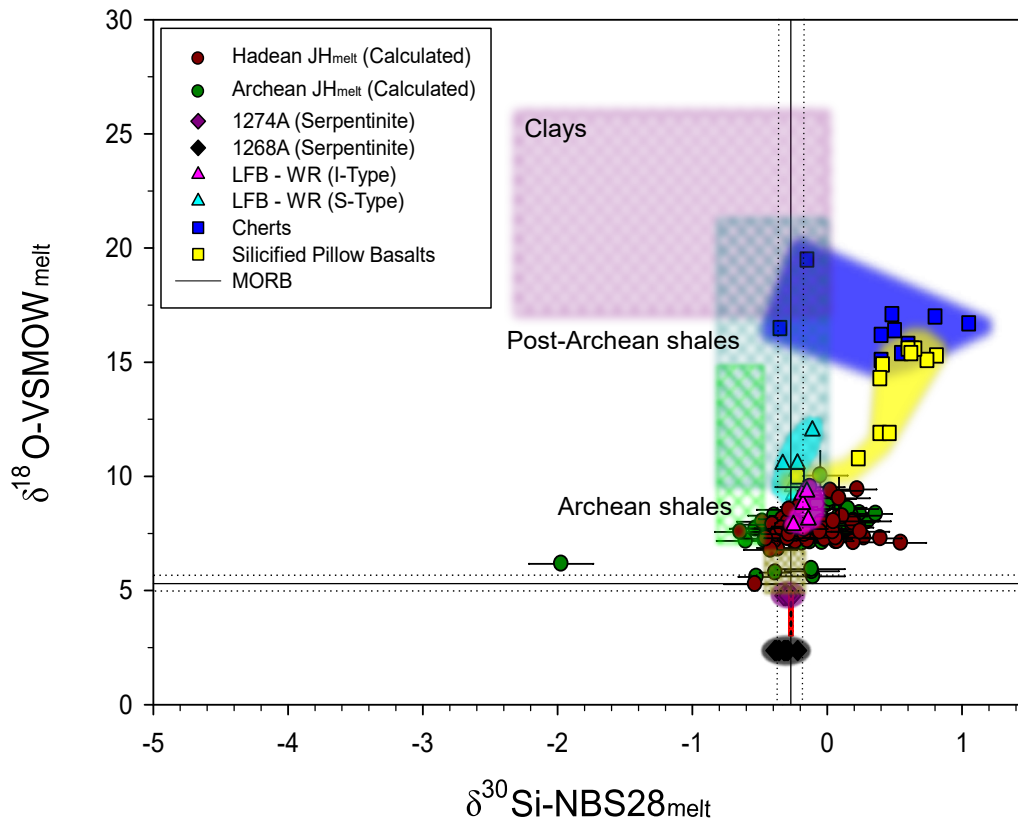


Figure 2. $\delta^{30}\text{Si}$ and $\delta^{18}\text{O}$ (± 2 s.e.; see online methods.) values of derived Hadean and Archean melts in comparison with Archean cherts/silicified pillow basalts from Barberton, South Africa³⁵ and modern ODP serpentinites ($\delta^{18}\text{O}^{36}$). Also shown are clays (dark pink box; $\delta^{30}\text{Si}^{37}$; $\delta^{18}\text{O}^{38}$), shales (Dark Cyan and green boxes; $\delta^{30}\text{Si}^{39}$; $\delta^{18}\text{O}^{40}$) OIBs (olive green box; $\delta^{30}\text{Si}$ of HIMU (Mangaia, Cook Islands), EM1 (Pitcairn islands) and EM2 (Samoa))⁴¹; $\delta^{18}\text{O}$ of EM1 and EM2⁴²; $\delta^{18}\text{O}$ of HIMU⁴² (Olivine phenocrysts⁴³, $\Delta^{18}\text{O}_{\text{melt-olivine}}^{44}$) representing HIMU, EM1 and EM2 mantle reservoirs and Archean komatiites (Red bar; $\delta^{30}\text{Si}$:^{126l}, $\delta^{18}\text{O}^{45, 46}$). JH_{melt} $\delta^{18}\text{O}$, serpentinite error bars are smaller than the symbols. The assimilation of these lithologies was also hinted at in just the JHZ isotopic data (Fig. S1). Data for MORB⁴⁷.

106 need to be invoked. We do so by comparing our calculated parent melts to modern granitoids from the
 107 Lachlan Fold Belt (LFB)²¹, clays, modern to Archean shales, Archean cherts, and Archean silicified
 108 pillow basalts. The mafic lithologies, sediments and cherts/silicified pillow basalts seem to suggest that
 109 these might be possible rocks that could have re-melted to create the composite melts from which the
 110 JHZs crystallized. The overlap between our melts and the Phanerozoic granitoids implies that some early
 111 Earth melts share chemical similarities with modern I-type granitoids. Although, when considering the
 112 isotopic values (low $\delta^{18}\text{O}$) for Archean shales, sediments like this could very well have been involved in
 113 the melting process, so S-type granitoid melts are also permissible when considering the isotope data.

114 If we compare the $\delta^{30}\text{Si}$ values of JHZ melts to recently reported values of Archaean rocks (Fig. 3A),
 115 there is overlap between our JHZ melts and Archaean cherts, silicified pillow basalts, TTGs, GMSs
 116 (Granite-Monzonite-Syenite) and komatiites, but the isotopic value of these Archaean rocks cannot
 117 explain the larger range in $\delta^{30}\text{Si}$ of all JHZ melts. They require lithologies with a large $\delta^{30}\text{Si}$ range²²⁻²⁴
 118 that may be assimilated to generate the melt values we derived. Archaean chert (Fig. 3A; grey crossed
 119 squares) is a possible lithology that might have been involved in shifting the $\delta^{30}\text{Si}$ values to greater-than
 120 mantle values given that, on balance, JHZ parent melt $\delta^{30}\text{Si}$ values are slightly heavier (Hadean: $-0.13 \pm$
 121 0.06 ‰ ; Archaean: $-0.14 \pm 0.09 \text{ ‰}$ (2 s.e.)) than the MORB reference ($\delta^{30}\text{Si} = -0.27 \text{ ‰}$). To test this
 122 observation, we performed two separate t-tests which compared the Hadean and Archaean $\delta^{30}\text{Si}$ values to
 123 the MORB reference and both tests showed that the Hadean and Archaean average $\delta^{30}\text{Si}$ values are
 124 statistically different from the MORB reference (see Online methods). This gives us a rare insight into

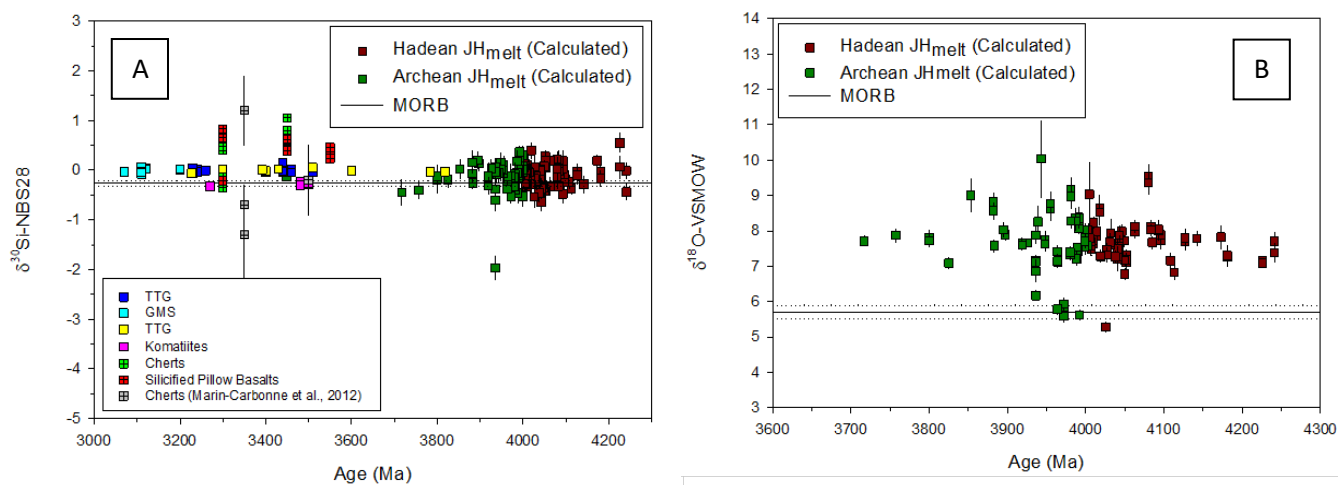


Figure 3A. $\delta^{30}\text{Si}$ of JH parent melts vs. age. The parent melts have been grouped by age. JH melts are compared to Archaean rocks. **B.** $\delta^{18}\text{O}$ of JH parent melts vs. age. In both graphs, the calculated isotopic composition of the Hadean and Archaean melts are statistically identical. **Data sources:** Cherts/Silicified pillow basalts^{23,36} (Green and red crossed squares; same data as Fig. 2 and Grey crossed squares); TTGs^{25, 26}; GMS²⁵; Komatiite²⁶; MORB⁴⁷.

125 what Hadean lithologies might have been. Similar arguments have been made to justify the $\delta^{30}\text{Si}$ values of
 126 Archean TTGs^{25, 26}.

127 Also, z-tests between the Hadean and the Archaean zircons (details in supplementary), show no statistical
128 difference between the Hadean and Archaean melt values in either isotopic (Fig. 3A & B) system. This
129 lack of a significant difference could imply that the geological processes and sources that gave the
130 Archaean JH parental melts their Si and O isotopic values (and SiO₂ content) began operating during the
131 Hadean.

132 Based on the inferences from our Si and O isotope models, sources involved in generating zircon-bearing
133 melts probably include cherts, serpentinites and chert/silicified pillow basalts. The involvement of these
134 source lithologies also imply the precipitation of cherts, low/high-T water-rock interaction to form
135 serpentinites and silicification of pillow basalts, their re-melting, and the evolution of the composite melt
136 to the point of zircon saturation all before the oldest zircon in our study crystallized (~4.2 Ga). A suitable
137 tectonic regime thus needs to account for all these processes as well as the possible constituent
138 lithologies. One possibility, among others¹⁷, is a plate-boundary regime that some liken to a modern
139 subduction zone⁶ where our proposed lithologies are recycled and interact with mantle reservoirs. Some
140 subduction zone properties implied by JHZs are that the JH parent melts may have been felsic, water-
141 saturated, similar in its volatile content to modern island arcs and formed in a low-T (650-800 °C), high-P
142 (>4 kbar) regime^{2, 7, 17, 27}. As a test for this possible formational regime, we compare our JHZ melt
143 TE/REE values to modern lavas.

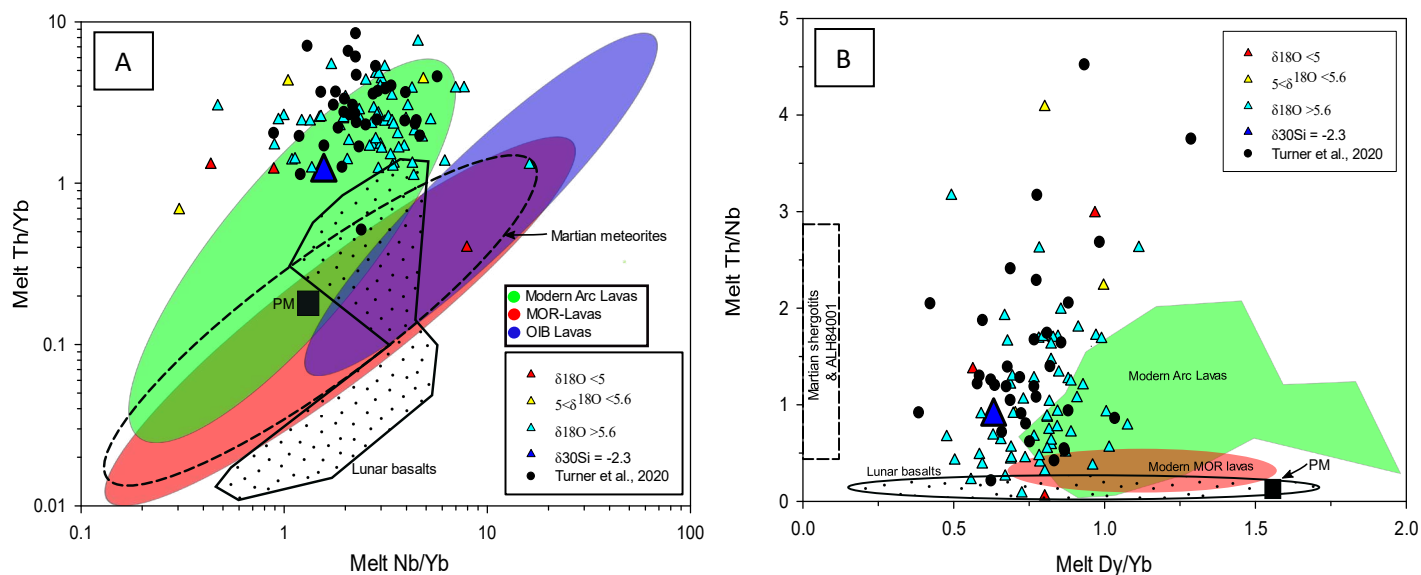


Figure 4 A & B: Comparison of elemental ratios of derived melt values between our JHZs (red, yellow, cyan and blue triangles) and those reported in [6] (black circles). **A:** Th-Nb proxy used to classify lavas from different regimes. Lunar and martian samples are shown as possible stagnant-lid regime analogues⁴⁸. **Field legend: Ocean Island Lavas (Blue), MOR lavas (Red), Modern arc lavas (Green).** **Data sources: Terrestrial lavas**^[31]; **Lunar basalts and martian meteorites**⁴⁸ **B:** Dy/Yb proxy for calc-alkaline differentiation as well as for restite garnet along with the Th/Nb proxy. **Data sources: MOR lavas**^[31]; **Modern arc lavas**^[32] **Martian meteorites**^[49, 50] **Lunar basalts**^[51]. **Primitive Mantle (PM; Black square)**^[52]. Trace element melt contents were derived from zircon using newly derived partition coefficients (see Extended data figures). Errors for our data are given in Table ST2.

144
 145 With the melt TE/REE values derived using our new partition coefficients, we compared JHZ melts to
 146 melt values proposed by [6] and compared JHZs of this study and from [6] to lavas from modern regimes
 147 where crust is generated on Earth, on discrimination diagrams (Fig. 4 A&B). We have also shown lunar
 148 basalts and martian meteorites fields as possible analogues for stagnant-lid tectonic scenarios with a
 149 caveat that these extra-terrestrial regimes might be anhydrous. These diagrams have been used to
 150 fingerprint tectonic settings of rocks and minerals²⁸⁻³². The Th/Nb proxy (Fig. 4A) is useful in
 151 differentiating between oceanic basalts and lavas with a continental input. Thorium and Nb have similar
 152 compatibility during partial melting of the mantle to form basalts, but continental input increases the Th
 153 content of melts. The Dy/Yb ratio (Fig. 4B) is used as a proxy for calc-alkaline differentiation as well as a
 154 proxy for garnet. SiO₂ % and Dy/Yb are negatively correlated while the crystallization of garnet increases
 155 the Dy/Yb ratio in the restite melt. Most of our melt values lie in the arc lava field in Fig. 4A, while in 4B

156 only some of them do so. They, however, do not fall in the MOR lava, lunar basalt or martian meteorite
157 fields. This implies that our JHZs and those of [6] were created in a regime that has chemical similarities
158 with modern arcs. We would like to mention that a system as complex as a subduction regime that
159 comprises several reservoirs such as fluxing fluids, mantle wedges, subducting slabs, sediments, etc. may
160 require multiple avenues of inquiry when attempting to define its signature chemistry and our study of
161 TEs, combined with isotopic measurements, presents one such avenue. One of the melts with lower-than-
162 mantle $\delta^{18}\text{O}$ zircon value falls in the mid-oceanic ridge field and so, may have originated in a setting
163 analogous to this. However, there are a couple of melts with greater-than-mantle $\delta^{18}\text{O}$ that also fall in this
164 field and some mantle-like $\delta^{18}\text{O}$ melts fall in the arc lava field. The majority of our datapoints are most
165 definitely chemically distinct from lunar basalts or martian meteorites. Even so, we find that JHZs
166 discussed here and in [6] strongly suggest formation in a regime with subduction zone-like chemical
167 characteristics. This observation and the dissimilarities with lunar and martian rocks places specific
168 chemical constraints on the JHZ formational environment and provides a limiting scenario about the
169 geodynamics of the early Earth.

170 We propose that water-rock interactions took place at the Earth's surface to generate Hadean cherts,
171 silicified pillow basalts and serpentinites. These lithologies were subsequently re-melted to generate
172 felsic, peraluminous/metaluminous melts based on Th/Y ratio and Al content. Moreover, these
173 interactions and re-melting processes gave the Hadean and the Archaean JHZs the same Si and O isotopic
174 content and thus might have been uniformly operating across these two eons. Finally, whatever the
175 precise details are of the regime that did create these zircons, our calculated WR compositions show clear
176 chemical similarities between it and modern plate boundaries. We are proposing naturally and
177 experimentally derived models that directly quantify the chemical and physical state of our planet during
178 its evolution during the first 500 to 700 Myr when life might have emerged³. This period of our planet is
179 important now; since we are exploring the habitability of other terrestrial-like planets some of which may
180 be like the Hadean Earth.

181

182

REFERENCES

183

1. Mojzsis, S. J., Harrison, T. M. & Pidgeon, R. T. Oxygen-isotope evidence from ancient zircons for liquid water at the Earth's surface 4,300 Myr ago. *Nature* **409**, 178-181, (2001).
- 184 2. Hopkins, M. D., Harrison, T. M. & Manning, C. E. Constraints on Hadean geodynamics from
185 mineral inclusions in > 4 Ga zircons. *Earth Planet. Sc. Lett.* **298**, 367-376 (2010).
- 186 3. Bell, E. A., Boehnke, P., Hopkins-Wielicki, M. D. & Harrison, T. M. Distinguishing primary
187 and secondary inclusion assemblages in Jack Hills zircons. *Lithos* **234-235**, 15-26, (2015).
- 188 4. Reimink, J. R., Davies, J. H. F. L., Bauer, A. M. & Chacko, T. A comparison between zircons
189 from the Acasta Gneiss Complex and the Jack Hills region. *Earth Planet. Sc. Lett.* **531**, (2020).
- 190 5. Trail, D., Bruce Watson, E. & Tailby, N. D. Ce and Eu anomalies in zircon as proxies for the
191 oxidation state of magmas. *Geochim. Cosmochim. Ac.* **97**, 70-87, (2012).
- 192 6. Turner, S., Wilde, S., Wörner, G., Schaefer, B. & Lai, Y.-J. An andesitic source for Jack Hills
193 zircon supports onset of plate tectonics in the Hadean. *Nat. Commun.* **11**, 1241-1245, (2020).
- 194 7. Chowdhury, W., Trail, D. & Bell, E. Boron partitioning between zircon and melt: Insights into
195 Hadean, modern arc, and pegmatitic settings. *Chem. Geol.* **551** (2020).
- 196 8. Bauer, A. M. *et al.* Hafnium isotopes in zircons document the gradual onset of mobile-lid
197 tectonics. *Geochem. Perspect. Let.* **14**, 1-6, (2020).
- 198 9. Van Kranendonk, M. J. *et al.* Making it thick: a volcanic plateau origin of Palaeoarchean
199 continental lithosphere of the Pilbara and Kaapvaal cratons. *Continent Formation through*
200 *Time* **389**, 83-111, doi:10.1144/Sp389.12 (2015).
- 201 10. O'Neill, C. & Debaille, V. The evolution of Hadean-Eoarchean geodynamics. *Earth Planet.*
202 *Sc. Lett.* **406**, 49-58, (2014).
- 203 11. Debaille, V. *et al.* Stagnant-lid tectonics in early Earth revealed by Nd-142 variations in late
204 Archean rocks. *Earth Planet. Sc. Lett.* **373**, 83-92 (2013).
- 205 12. Sleep, N. H., Zahnle, K. J. & Lupu, R. E. Terrestrial aftermath of the Moon-forming impact.
206 *Philos. T. R. Soc. A.* **372** (2014).
- 207 13. Foley, B. J. & Rizo, H. Long-term preservation of early formed mantle heterogeneity by
208 mobile lid convection: Importance of grainsize evolution. *Earth Planet. Sc. Lett.* **475**, 94-105,
209 (2017).
- 210 14. Rosas, J. C. & Korenaga, J. Rapid crustal growth and efficient crustal recycling in the early
211 Earth: Implications for Hadean and Archean geodynamics. *Earth Planet. Sc. Lett.* **494**, 42-49,
212 (2018).
- 213 15. Korenaga, J. Crustal evolution and mantle dynamics through Earth history. *Philos. T. R. Soc.*
214 *A.* **376** (2018).
- 215 16. Aarons, S. M. *et al.* Titanium isotopes constrain a magmatic transition at the Hadean-Archean
216 boundary in the Acasta Gneiss Complex. *Sci. Adv.* **6**, (2020).
- 217 17. Harrison T. M. (2020), *Hadean Earth*, Springer, Cham, Switzerland,
218 <https://doi.org/10.1007/978-3-030-46687-9>.
- 219 18. Ferry, J. M. & Watson, E. B. New thermodynamic models and revised calibrations for the Ti-
220 in-zircon and Zr-in-rutile thermometers. *Contrib. Mineral. Petr.* **154**, 429-437 (2007).
- 221 19. Trail, D., Savage, P. S. & Moynier, F. Experimentally determined Si isotope fractionation
222 between zircon and quartz. *Geochim. Cosmochim. Ac.* **260**, 257-274 (2019).
- 223 20. Lackey, J. S., Valley, J. W., Chen, J. H. & Stockli, D. F. Dynamic Magma Systems, Crustal
224 Recycling, and Alteration in the Central Sierra Nevada Batholith: The Oxygen Isotope Record.
225 *J. Petrol.* **49**, 1397-1426 (2008).
- 226

- 227 21. Savage, P. S., Georg, R. B., Williams, H. M., Burton, K. W. & Halliday, A. N. Silicon isotope
228 fractionation during magmatic differentiation. *Geochim. Cosmochim. Ac.* **75**, 6124-6139
229 (2011).
- 230 22. Robert, F. & Chaussidon, M. A palaeotemperature curve for the Precambrian oceans based on
231 silicon isotopes in cherts. *Nature* **443**, 969-972 (2006).
- 232 23. Marin-Carbonne, J., Chaussidon, M. & Robert, F. Micrometer-scale chemical and isotopic
233 criteria (O and Si) on the origin and history of Precambrian cherts: Implications for paleo-
234 temperature reconstructions. *Geochim. Cosmochim. Ac.* **92**, 129-147 (2012).
- 235 24. Andre, L., Cardinal, D., Alleman, L. Y. & Moorbath, S. Silicon isotopes in 3.8 Ga West
236 Greenland rocks as clues to the Eoarchaeon supracrustal Si cycle. *Earth Planet. Sc. Lett.* **245**,
237 162-173 (2006).
- 238 25. Andre, L. *et al.* Early continental crust generated by reworking of basalts variably silicified by
239 seawater. *Nat. Geosci.* **12**, 769 (2019).
- 240 26. Deng, Z. B. *et al.* An oceanic subduction origin for Archaean granitoids revealed by silicon
241 isotopes. *Nat. Geosci.* **12**, 774 (2019).
- 242 27. Trail, D. *et al.* Constraints on Hadean zircon protoliths from oxygen isotopes, Ti-thermometry,
243 and rare earth elements. *Geochem. Geophys. Geosy.* **8** (2007).
- 244 28. Sun, S. s. & McDonough, W. F. Chemical and isotopic systematics of oceanic basalts:
245 implications for mantle composition and processes. *Geological Society, London, Special*
246 *Publications* **42**, 313 (1989).
- 247 29. Pearce, J. A. & Peate, D. W. Tectonic Implications of the Composition of Volcanic ARC
248 Magmas. *Annu. Rev. Earth. Pl. Sc.* **23**, 251-285 (1995).
- 249 30. Pearce, J. A. Geochemical fingerprinting of oceanic basalts with applications to ophiolite
250 classification and the search for Archean oceanic crust. *Lithos* **100**, 14-48, (2008).
- 251 31. Davidson, J., Turner, S. & Plank, T. Dy/Dy*: Variations Arising from Mantle Sources and
252 Petrogenetic Processes. *J. Petrol.* **54**, 525-537 (2013).
- 253 32. Grimes, C. B., Wooden, J. L., Cheadle, M. J. & John, B. E. "Fingerprinting" tectono-
254 magmatic provenance using trace elements in igneous zircon. *Contrib. Mineral. Petr.* **170**, 46,
255 (2015).
- 256 33. Burnham, A. D. & Berry, A. J. An experimental study of trace element partitioning between
257 zircon and melt as a function of oxygen fugacity. *Geochim. Cosmochim. Ac.* **95**, 196-212,
258 (2012).
- 259 34. Rudnick, R. L. & Gao, S. in *Treatise on Geochemistry* (eds Heinrich D. Holland & Karl K.
260 Turekian) 1-64 (Pergamon, 2003).
- 261 35. Abraham, K. *et al.* Coupled silicon-oxygen isotope fractionation traces Archaean silicification.
262 *Earth Planet. Sc. Lett.* **301**, 222-230 (2011).
- 263 36. Barnes, J. D., Paulick, H., Sharp, Z. D., Bach, W. & Beaudoin, G. Stable isotope ($\delta^{18}\text{O}$, δD ,
264 $\delta^{37}\text{Cl}$) evidence for multiple fluid histories in mid-Atlantic abyssal peridotites (ODP Leg 209).
265 *Lithos* **110**, 83-94 (2009).
- 266 37. Douthitt, C. B. The geochemistry of the stable isotopes of silicon. *Geochimica et*
267 *Cosmochimica Acta* **46**, 1449-1458 (1982).
- 268 38. Bindeman, I. Oxygen Isotopes in Mantle and Crustal Magmas as Revealed by Single Crystal
269 Analysis. *Reviews in Mineralogy and Geochemistry* **69**, 445-478 (2008).
- 270 39. Savage, P., Georg, B., Williams, H. & Halliday, A. The silicon isotope composition of the
271 upper continental crust. *Geochim. Cosmochim. Ac.* **109**, 384-399 (2013).
- 272 40. Bindeman, I. N., Bekker, A. & Zakharov, D. O. Oxygen isotope perspective on crustal
273 evolution on early Earth: A record of Precambrian shales with emphasis on Paleoproterozoic
274 glaciations and Great Oxygenation Event. *Earth Planet. Sc. Lett.* **437**, 101-113 (2016).

- 275 41. Pringle, E. A. *et al.* Silicon isotopes reveal recycled altered oceanic crust in the mantle sources
276 of Ocean Island Basalts. *Geochim. Cosmochim. Ac.* **189**, 282-295 (2016).
- 277 42. Harmon, R. S. & Hoefs, J. Oxygen isotope heterogeneity of the mantle deduced from global
278 ¹⁸O systematics of basalts from different geotectonic settings. *Contrib. Mineral. Petr.* **120**, 95-
279 114 (1995).
- 280 43. Eiler, J. M. *et al.* Oxygen isotope variations in ocean island basalt phenocrysts. *Geochim.*
281 *Cosmochim. Ac.* **61**, 2281-2293 (1997).
- 282 44. Bindeman, I., A. Gurenko, O. Sigmarsson & M. Chaussidon. Oxygen isotope heterogeneity
283 and disequilibria of olivine crystals in large volume Holocene basalts from Iceland: Evidence
284 for magmatic digestion and erosion of Pleistocene hyaloclastites. *Geochim. Cosmochim.*
285 *Ac.* **72**, 4397-4420 (2008).
- 286 45. Byerly, B. L., Kareem, K., Bao, H. & Byerly, G. R. Early Earth mantle heterogeneity revealed
287 by light oxygen isotopes of Archaean komatiites. *Nat. Geosci.* **10**, 871-875 (2017).
- 288 46. Lécuyer, C., gruau, G., Anhaeusser, C. R. & Fourcade, S. The origin of fluids and the effects
289 of metamorphism on the primary chemical compositions of Barberton komatiites: New
290 evidence from geochemical (REE) and isotopic (Nd, O, H, ³⁹Ar-⁴⁰Ar) data. *Geochim.*
291 *Cosmochim. Ac.* **58**, 969-984, (1994).
- 292 47. Savage, P. S., Georg, R. B., Armytage, R. M. G., Williams, H. M. & Halliday, A. N. Silicon
293 isotope homogeneity in the mantle. *Earth Planet. Sc. Lett.* **295**, 139-146, (2010).
- 294 48. Condie, K. C. & Shearer, C. K. Tracking the evolution of mantle sources with incompatible
295 element ratios in stagnant-lid and plate-tectonic planets. *Geochim. Cosmochim. Ac.* **213**, 47-
296 62, (2017).
- 297 49. Taylor, L. A., et al., Martian meteorite Dhofar 019: A new shergottite. *Meteoritics &*
298 *Planetary Science* **37**, 1107-1128 (2002)
- 299 50. Meyer C. 2009. the Mars meteorite compendium. ([http://www-
300 curator.jsc.nasa.gov/antmet/mmc/](http://www-curator.jsc.nasa.gov/antmet/mmc/)).
- 301 51. Hallis, L. J., M. Anand & S. Strekopytov. Trace-element modelling of mare basalt parental
302 melts: Implications for a heterogeneous lunar mantle. *Geochim. Cosmochim. Ac.* **134**: 289-
303 316 (2014).
- 304 52. Lyubetskaya, T. and J. Korenaga. Chemical composition of Earth's primitive mantle and its
305 variance: 1. Method and results. *J. Geophys. Res.: Solid Earth* **112**(B3). (2007).
- 306
- 307

Supplementary Files

This is a list of supplementary files associated with this preprint. Click to download.

- [Onlinemethods.docx](#)
- [Supplementaryinformation.docx](#)
- [Supplementarytables.xlsx](#)
- [Extendeddatafigures.docx](#)